Imaging Proliferation in Lung Tumors with PET: ^{18}F-FLT Versus ^{18}F-FDG

Andreas K. Buck, MD[1]; Gisela Halter, MD[2]; Holger Schirrmeister, MD[1]; Jörg Kotzerke, MD[1]; Imke Wurziger[2]; Gerhard Glatting, PhD[1]; Torsten Mattfeldt, MD[3]; Bernd Neumaier, PhD[1]; Sven N. Reske, MD[1]; and Martin Hetzel, MD[4]

[1]Department of Nuclear Medicine, University of Ulm, Ulm, Germany; [2]Department of Thoracic Surgery, University of Ulm, Ulm, Germany; [3]Department of Pathology, University of Ulm, Ulm, Germany; and [4]Department of Internal Medicine II, University of Ulm, Ulm, Germany

Recently, the thymidine analog 3′-deoxy-3′-^{18}F-fluorothymidine (FLT) was suggested for imaging tumoral proliferation. In this prospective study, we examined whether ^{18}F-FLT better determines proliferative activity in newly diagnosed lung nodules than does ^{18}F-FDG. **Methods:** Twenty-six patients with pulmonary nodules on chest CT were examined with PET and the tracers ^{18}F-FDG and ^{18}F-FLT. Tumoral uptake was determined by calculation of standardized uptake value (SUV). Within 2 wk, patients underwent resective surgery or had core biopsy. Proliferative activity was estimated by counting nuclei stained with the Ki-67–specific monoclonal antibody MIB-1 per total number of nuclei in representative tissue specimens. The correlation between the percentage of proliferating cells and the SUVs for ^{18}F-FLT and ^{18}F-FDG was determined using linear regression analysis. **Results:** Eighteen patients had malignant tumors (13 with non–small cell lung cancer [NSCLC], 1 with small cell lung cancer, and 4 with pulmonary metastases from extrapulmonary tumors); 8 had benign lesions. In all visible lesions, mean ^{18}F-FDG uptake was 4.1 (median, 4.4; SD, 3.0; range, 1.0–10.6), and mean ^{18}F-FLT uptake was 1.8 (median, 1.2; SD, 2.0; range, 0.8–6.4). Statistical analysis revealed a significantly higher uptake of ^{18}F-FDG than of ^{18}F-FLT (Mann–Whitney *U* test, $P < 0.05$). ^{18}F-FLT SUV correlated better with proliferation index ($P < 0.0001$; $r = 0.92$) than did ^{18}F-FDG SUV ($P < 0.001$; $r = 0.59$). With the exception of 1 carcinoma in situ, all malignant tumors showed increased ^{18}F-FDG PET uptake. ^{18}F-FLT PET was false-negative in the carcinoma in situ, in another NSCLC with a low proliferation index, and in a patient with lung metastases from colorectal cancer. Increased ^{18}F-FLT uptake was related exclusively to malignant tumors. By contrast, ^{18}F-FDG PET was false-positive in 4 of 8 patients with benign lesions. **Conclusion:** ^{18}F-FLT uptake correlates better with proliferation of lung tumors than does uptake of ^{18}F-FDG and might be more useful as a selective biomarker for tumor proliferation.

Key Words: ^{18}F-FLT; ^{18}F-FDG; Ki-67; proliferation; lung cancer

J Nucl Med 2003; 44:1426–1431

Received Nov. 27, 2002; revision accepted Feb. 19, 2003.

For correspondence or reprints contact: Andreas K. Buck, MD, Department of Nuclear Medicine, University of Ulm, Robert-Koch-Strasse 8, D-89081 Ulm, Germany.

E-mail: andreas.buck@medizin.uni-ulm.de

PET using the glucose analog ^{18}F-FDG enables noninvasive tissue characterization based on metabolic differences between benign and malignant tumors. Several studies have found ^{18}F-FDG PET to have a high sensitivity for staging lung cancer (*1–3*). However, ^{18}F-FDG uptake is not tumor specific, and false-positive findings can occur in inflammatory lesions (*4*). Therefore, many efforts have been made to develop more selective tracers. In contrast to ^{18}F-FDG uptake values, proliferative activity as measured by Ki-67 immunostaining has been shown to be a specific sign of malignant tumors (*5*). Furthermore, immunohistochemical studies using various biomarkers for proliferation showed significantly decreased survival in patients with highly proliferating tumors (*6*). In clinical studies, ^{18}F-FDG uptake correlated with proliferative activity (*7,8*) and survival in non–small cell lung cancer (NSCLC) (*9,10*).

^{11}C-Thymidine was the first radiotracer for noninvasive imaging of tumor proliferation (*11*). The short half-life of ^{11}C and rapid metabolism of ^{11}C-thymidine in vivo make the radiotracer less suitable for routine use. Hence, the thymidine analog 3′-deoxy-3′-^{18}F-fluorothymidine (FLT) was recently introduced as a stable proliferation marker with a suitable nuclide half-life (*12*). ^{18}F-FLT is phosphorylated to 3′-fluorothymidine monophosphate by thymidine kinase 1 and reflects thymidine kinase 1 activity in A549 lung cancer cells (*13*). In a first clinical study, our group demonstrated proliferation-dependent ^{18}F-FLT uptake in NSCLC (*14*).

We devised a prospective study to evaluate whether PET with the novel tracer ^{18}F-FLT better determines tumoral proliferation and better differentiates benign from malignant lung tumors than does PET with ^{18}F-FDG.

MATERIALS AND METHODS

Patients

This prospective study included 26 patients (17 men, 9 women) with a mean age of 62 ± 9.9 y (range, 37–77 y; Table 1). PET with both tracers, ^{18}F-FDG and ^{18}F-FLT, was planned for 30 consecutive patients. Four patients had to be excluded from the study because only ^{18}F-FDG or ^{18}F-FLT PET was performed. Patients were selected when pulmonary nodules on CT scans strongly

TABLE 1
Patient Characteristics, Tumoral Tracer Uptake, and Proliferation Fraction (Ki-67 Index)

Patient no.	Age (y)	Sex	Histopathology finding	TNM	SUV				Ki-67 index (%)
					^{18}F-FLT		^{18}F-FDG		
					Mean	Maximum	Mean	Maximum	
1	57	F	Non–small cell lung cancer	T1 N1 M0	5.6	8.7	6.3	11.3	65
2	53	M	Non–small cell lung cancer	T2 N1 M0	4.0	5	7.6	13.5	41
3	77	F	Non–small cell lung cancer	T2 N1 M0	4.0	5.3	10.6	22.7	43
4	71	F	Non–small cell lung cancer	T2 N1 M0	2.9	4.4	4.13	6.5	35
5	75	M	Non–small cell lung cancer	T2b N0 M0	3.1	5.7	6.5	12.5	54
6	53	F	Non–small cell lung cancer	T2 N1 M0	Neg	Neg	2.6	3.1	10
7	61	M	Non–small cell lung cancer	T3 N0 M0	4.9	6.8	5.1	7.3	45
8	76	M	Non–small cell lung cancer	T4 N2 M0	3.1	5.2	7.9	12.3	35
9	55	M	Non–small cell lung cancer	T2 N2 MX	3.9	5.6	6.8	11	40
10	62	F	Non–small cell lung cancer	TX N0 M0	2.3	3.3	4.6	7.3	10
11	55	M	Non–small cell lung cancer	T1 N1 M0	1.1	1.3	5.5	10.1	12
12	56	F	Non–small cell lung cancer	T3 N3 M0	6.4	10.4	4.8	8.3	70
13	67	M	Non–small cell lung cancer (carcinoma in situ)	T1 N0 M0	Neg	Neg	Neg	Neg	32
14	66	M	Small cell lung cancer	T4 N2 M0	1.7	2.4	7.3	12.7	20
15	68	M	Met from colorectal cancer	rTX N0 M1	Neg	Neg	3.7	6.8	12
16	51	M	Met from renal cell carcinoma	rTX N0 M1	2.1	3.4	6.7	12.1	23
17	65	M	Met from renal cell carcinoma	rTX N0 M1	1.3	1.9	1.0	1.4	10
18	37	F	Met from osteosarcoma	TX N0 M1	0.8	1	1.5	1.5	1
19	75	M	Bronchiolitis	—	Neg	Neg	6.9	10.3	0
20	76	M	2 × 3 cm nodule, benign lesion indicated by clinical course	—	Neg	Neg	3.0	4.3	0
21	51	F	Tuberculoma	—	Neg	Neg	1.1	1.8	5
22	59	M	Bronchiolitis	—	Neg	Neg	Neg	Neg	0
23	69	M	Bronchiolitis	—	Neg	Neg	Neg	Neg	0
24	67	M	1 × 2 cm nodule, benign lesion indicated by clinical course	—	Neg	Neg	2.2	2.9	0
25	55	F	Fibroma	—	Neg	Neg	Neg	Neg	0
26	56	M	Chondroma	—	Neg	Neg	Neg	Neg	0

Neg = negative; met = metastasis.

suggested a malignant tumor. Sixteen patients underwent resective surgery up to 14 d after ^{18}F-FLT and ^{18}F-FDG PET. In the other 10 patients, core-biopsy specimens were used for histopathologic evaluation. All patients gave written consent to participate in this study, which was approved by the local ethical committee.

Eighteen patients had malignant tumors. Histopathologic examination revealed NSCLC in 13 patients; small cell lung cancer in 1 patient; and pulmonary metastases from colorectal cancer, renal cell carcinoma, or osteosarcoma in 4 patients. Eight patients had benign tumors (1 case of bronchopulmonary chondroma; 3 of bronchiolitis; 1 of tuberculoma; 1 of focal fibrosis; and 2 of undefined tumors, for which malignancy was excluded by the clinical course).

Immunostaining and Morphometric Analysis

The detailed protocol for immunostaining was published elsewhere (*5*). Briefly, formalin-fixed and paraffin-embedded sections (5 μm) of resected specimens and biopsy samples were dewaxed, rehydrated, and microwaved in 0.01 mol/L citrate buffer for 30 min. For immunostaining, the monoclonal murine antibody MIB-1 (Dianova), specific for human nuclear antigen Ki-67, was used in a 1:500 dilution. Sections were lightly counterstained with hematoxylin. As a positive control for proliferating cells, sections of human lymph node tissue were used. The primary antibody was omitted on sections used as negative controls. Histopathologic slides were examined by a pathologist who was unaware of the patients' clinical data.

An area with high cellularity was chosen for the evaluation of MIB-1 immunostaining. All epithelial cells with nuclear staining of any intensity were defined as positive. Proliferative activity was described as the percentage of MIB-1–stained nuclei per total number of nuclei in the sample. With light microscopy, 600 nuclei per slide and 3 slides per case were evaluated for Ki-67 expression to minimize tissue-sampling error. Representative images of each slide were transferred to the computer frame by a video camera using the computer-assisted imaging system OPTIMAS 6.2 (Media Cybernetics, Inc.).

^{18}F-FLT Synthesis and PET Imaging

In accord with the method of Machulla et al. (*15*), benzoyl-protected anhydrothymidine was used for ^{18}F-FLT synthesis. Radiosynthesis was performed in a PET tracer synthesizer from nuclear interface. After nucleophilic introduction of ^{18}F-fluoride accompanied by an anhydro-ring opening, the benzylated intermediate was cleaved using 1% NaOH solution. ^{18}F-FLT was purified via preparative high-performance liquid chromatography.

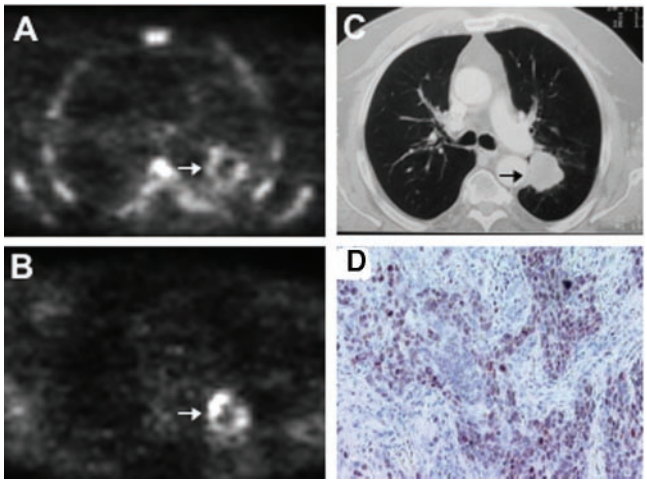

FIGURE 1. Patient 5, with NSCLC in left upper lobe. (A) Transaxial ^{18}F-FLT PET scan demonstrates high ^{18}F-FLT uptake (arrow) in tumor margin. ^{18}F-FLT uptake in vertebral column, scapula, and ribs represents proliferating bone marrow. (B and C) Corresponding ^{18}F-FDG PET and CT scans show high ^{18}F-FDG uptake in tumor margin and primary lung tumor. (D) On Ki-67 immunohistochemistry, Ki-67–positive nuclei (brown) demonstrate high proliferation rate of 54%, and hematoxylin background staining reveals Ki-67–negative nuclei (blue).

^{18}F-FLT and ^{18}F-FDG PET examinations were performed on consecutive days within 2 wk before resective surgery or core biopsy. PET was performed using a high-resolution full-ring scanner (ECAT EXACT or ECAT HR+; Siemens/CTI), which produces 47 or 63 contiguous slices per bed position. Axial field of view is 15.5 cm per bed position. Five bed positions were measured for each patient, covering a total field of view of 77.5 cm. The emission scan included the thorax and abdomen for all patients. Patients fasted for at least 6 h before undergoing PET. Static emission scans were obtained 45 min after injection of 265–370 MBq of ^{18}F-FLT (mean, 334 MBq) or 345–550 MBq of ^{18}F-FDG (mean, 391 MBq). The acquisition time was 10 min per bed position. Four-minute transmission scans with a ^{68}Ge/^{68}Ga ring source were obtained for attenuation correction after tracer application. Images were reconstructed using an iterative reconstruction algorithm described by Schmidlin (*16*).

All images were evaluated by 2 experienced nuclear medicine physicians. For calculation of standardized uptake value (SUV), circular regions of interest were drawn containing the area with focally increased pulmonary ^{18}F-FLT and ^{18}F-FDG uptake (lesional diameter at spiral CT, 4–48 mm).

Data Analysis

Data are presented as mean, median, range, and SD. The amount of Ki-67–positive cells and the SUVs for ^{18}F-FDG and ^{18}F-FLT were compared using linear regression analysis. Differences were considered statistically significant at $P < 0.05$. ^{18}F-FDG and ^{18}F-FLT uptakes were compared using the Mann–Whitney *U* test.

RESULTS

^{18}F-FDG PET

All malignant lesions except 1 carcinoma in situ (NSCLC, patient 13) showed focally increased and easily detectable ^{18}F-FDG uptake (Table 1). The mean ^{18}F-FDG SUV in all visible lesions was 4.1 (median, 4.4; SD, 3.0; range, 1.0–10.6). The mean maximum ^{18}F-FDG uptake was 6.9 (median, 7.0; SD, 5.8; range, 1.4–22.7).

The mean ^{18}F-FDG SUV in the 13 patients with NSCLC was 5.6 (median, 5.5; SD, 2.6; range, 1.0–10.6; Fig. 1), and the mean maximum ^{18}F-FDG SUV was 9.7 (median, 10.1; SD, 5.5; range, 1.4–22.7). Four of the 8 patients with benign lesions presented with focal ^{18}F-FDG uptake. The reviewers visually interpreted 2 of 8 nodules as malignant. Histopathologic examination revealed unifocal tuberculoma in one patient (patient 21; mean ^{18}F-FDG SUV, 1.1; maximum ^{18}F-FDG SUV, 1.8; Fig. 2) and focal bronchiolitis in another patient (patient 19; mean ^{18}F-FDG SUV, 6.9; maximum ^{18}F-FDG SUV, 10.3). Inflammatory lesions were suspected in the other 2 patients. Tissue sampling was not performed because clinical follow-up at 3 mo indicated benign lesions (a 1 × 2 cm nodule disappeared on CT performed at the 3-mo follow-up examination, and a 2 × 3 cm nodule decreased to 1 × 1 cm). Mean ^{18}F-FDG SUVs in these lesions were 2.2 and 3.0, respectively, and maximum ^{18}F-FDG SUVs were 2.9 and 4.3, respectively.

^{18}F-FLT PET

The mean ^{18}F-FLT SUV in all visible lesions was 1.8 (median, 1.2; SD, 2.0; range, 0.8–6.4; Table 1), and the mean maximum ^{18}F-FLT SUV was 2.7 (median, 1.6; SD, 3.1; range, 1.3–10.4). Mean ^{18}F-FLT SUV in NSCLC was 3.2 (median, 3.1; SD, 2.0; range, 0.8–6.4), and the mean maximum ^{18}F-FLT SUV was 4.7 (median, 5.2; SD, 3.1; range, 1.0–10.4). Increased ^{18}F-FLT uptake within a nodule was identified in 11 of 13 patients with histologically confirmed NSCLC (Fig. 1). Patient 6, with highly differentiated

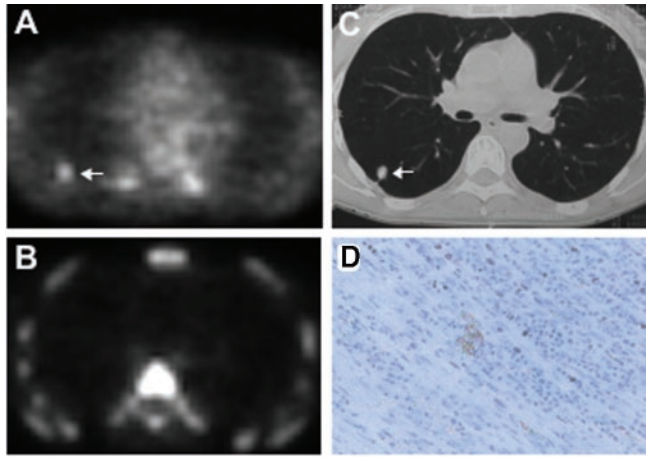

FIGURE 2. Patient 21, with history of colorectal cancer and suggestive nodule in right middle lobe, for which histopathology revealed solitary tuberculoma. (A) Transaxial ^{18}F-FDG PET scan demonstrates moderate ^{18}F-FDG uptake (arrow) in tumor. (B) No focal tracer accumulation is seen in corresponding ^{18}F-FLT PET scan. (C) Corresponding CT scan shows pulmonary nodule in right middle lobe. (D) On Ki-67 immunohistochemistry, 5% of nuclei show immunoreactivity to Ki-67 antigen.

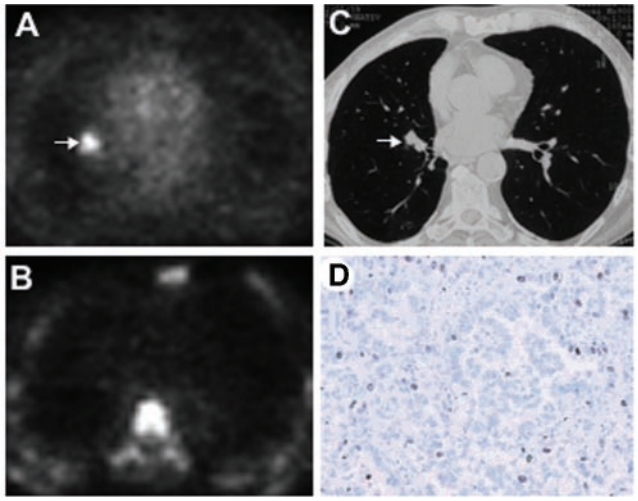

FIGURE 3. Patient 15, with pulmonary metastases from colorectal cancer. (A) Transaxial ^{18}F-FDG PET scan demonstrates high ^{18}F-FDG uptake (B) in metastatic nodule in right middle lobe. (B) ^{18}F-FLT PET scan shows no tumoral ^{18}F-FLT accumulation. (C) Corresponding CT scan shows pulmonary nodule in right middle lobe. (D) On Ki-67 immunohistochemistry, 12% of nuclei exhibit immunoreactivity to Ki-67–specific antibody MIB-1, indicating low proliferative activity.

NSCLC and a low proliferation fraction, and patient 13, with a carcinoma in situ, had no visible ^{18}F-FLT uptake.

In pulmonary metastases, the mean ^{18}F-FLT SUV was 1.1 (median, 1.3; SD, 0.8; range, 0.8–2.1), and the mean maximum ^{18}F-FLT SUV was 1.6 (median, 1.9; SD, 1.3; range, 1.0–3.4). In the 1 patient with pulmonary metastases from colorectal cancer (patient 15), the metastases showed no ^{18}F-FLT uptake (Fig. 3). Another patient, with small cell lung cancer (patient 14), showed weak but easily detectable ^{18}F-FLT uptake (mean ^{18}F-FLT SUV, 1.7). No benign tumors showed focal ^{18}F-FLT uptake. Hence, SUV was not determined for these tumors.

In all pulmonary lesions, mean and maximum ^{18}F-FLT uptake was lower than the respective ^{18}F-FDG uptake. Mean ^{18}F-FLT SUV was significantly lower than the respective ^{18}F-FDG SUV (Mann–Whitney U test, $P < 0.05$). The mean maximum SUVs of ^{18}F-FDG were also significantly higher ($P < 0.0001$).

Ki-67 Immunohistochemistry

Regional lymph nodes serving as a positive control showed an intense nuclear staining with Ki-67 antibody. In control sections, for which the primary antibody was omitted, no positive nuclear staining was visible.

All malignant tissue specimens contained Ki-67–positive cells. Stained nuclei belonged mainly to epithelial cells, and a very small portion belonged to inflammatory cells. Ki-67 positivity ranged from 1% to 70% of sampled epithelial nucleus profiles (median, 35%). The mean fraction of Ki-67–positive nuclei was 33% (SD, 6.5%). In 6 cases, more than 40% of nuclei showed immunoreactivity for Ki-67 antigen. In NSCLC, the mean proliferation fraction was 37.8% (median, 40%; SD, 19.1%; range, 10%–70%). In pulmonary metastases, the mean proliferative fraction was lower (11.5%; median, 11%; SD, 9%; range, 1%–23%).

Ki-67–positive cells were present in only 1 specimen with benign disease (patient 21, with tuberculoma; Ki-67 index, 5%). Seven benign tissue specimens showed no immunoreactivity to Ki-67 antigen. The range for Ki-67–positive cells was 0%–5%. Ki-67–positive nuclei belonged mainly to inflammatory cells rather than to epithelial cells. The mean of Ki-67–positive cells in benign lesions was 1% (SD, 1.4).

In all lung tumors, linear regression analysis indicated a highly significant correlation between ^{18}F-FLT SUV and

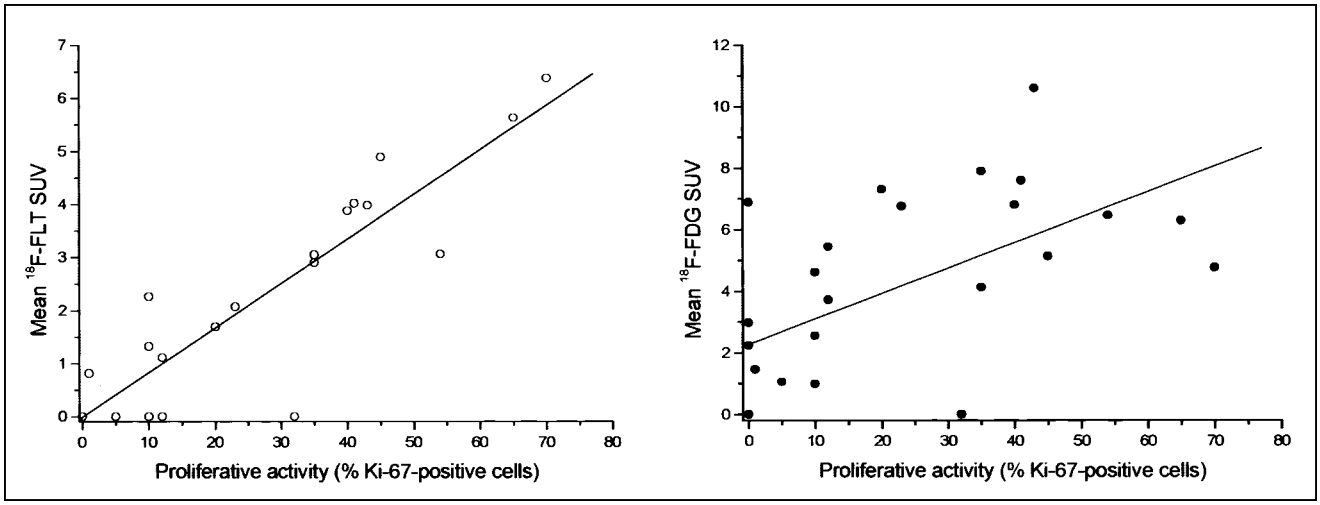

FIGURE 4. Linear regression analysis of mean tumoral SUVs of ^{18}F-FLT and ^{18}F-FDG and proliferation fraction (percentage of Ki-67–positive tumor cells). Mean ^{18}F-FLT SUV: significant correlation for $P < 0.0001$, $r = 0.92$. Mean ^{18}F-FDG SUV: significant correlation for $P < 0.001$, $r = 0.59$.

Ki-67 index ($P < 0.0001$; $r = 0.92$; Fig. 4). Between Ki-67 and ^{18}F-FDG SUV, statistical analysis also revealed a significant correlation ($P < 0.001$; Fig. 4) but a weak correlation coefficient ($r = 0.59$).

DISCUSSION

This is the first clinical study comparing the correlation between ^{18}F-FDG uptake and proliferation rate and the correlation between ^{18}F-FLT and proliferation rate for unclear lung lesions. Compared with conventional imaging modalities, ^{18}F-FDG PET has been reported to offer the highest sensitivity for staging lung cancer (*17,18*). In agreement with these findings, ^{18}F-FDG uptake was increased in all malignant tumors except 1 carcinoma in situ (in patient 13) in our series.

Despite high sensitivity, false-positive findings can occur with ^{18}F-FDG PET, especially in inflammatory lesions (*4*). Concordantly, focal ^{18}F-FDG uptake was present in 4 of our study patients with inflammatory or other benign lesions (1 case of bronchiolitis, 1 of tuberculoma, and 2 of undefined benign lung tumors). The relatively high number of false-positive findings in the present series is related to patient selection. Other studies with more patients found specificities averaging 78% for ^{18}F-FDG PET in detecting lung cancer (*3*). Recently, unspecific ^{18}F-FDG uptake has been reported in inflammatory cells such as macrophages (*19*). Furthermore, many other factors have been reported to influence ^{18}F-FDG uptake, such as upregulation of glucose transporter 1 receptors (*20,21*), number of viable tumor cells (*22*), microvessel density, or hexokinase expression (*23*). In pancreatic cancer, we previously demonstrated that proliferation was a specific sign for malignancy (*5*) and clearly differentiated benign from malignant tumors. Therefore, a marker specific for proliferation could reduce false-positive PET findings.

A significant correlation between ^{18}F-FDG uptake and proliferative activity was also found for breast cancer (*24*) and NSCLC (*7*). However, the low correlation coefficient ($r = 0.41–0.73$) indicated that ^{18}F-FDG uptake reflects proliferation only in part. In agreement with these findings, the correlation coefficient was as low as 0.59 ($r^2 = 0.35$) in our study. That means that only 35% of ^{18}F-FDG uptake in lung tumors can be explained by proliferative activity.

Various nucleoside analogs have been assessed for imaging proliferation (*25–27*), but ^{18}F-FLT is probably the best approach so far. ^{18}F-FLT turned out to be stable in vivo (*12*) and accumulates in lung cancer cells in a proliferation-dependent manner (*13*). Furthermore, thymidine kinase 1 was revealed as the key enzyme responsible for intracellular trapping of ^{18}F-FLT (*28*). However, the detailed uptake mechanism is still unknown, and the influence of other factors, such as expression of nucleoside transporters, remains to be determined.

For patients with pulmonary nodules, our data show a highly significant correlation between tumoral ^{18}F-FLT uptake and proliferative activity as indicated by Ki-67 immunostaining. The correlation coefficient was 0.92 ($r^2 = 0.85$). In contrast to the lower correlation coefficient observed for ^{18}F-FDG, 85% of tracer uptake can be explained by proliferative activity. In agreement with this finding, no ^{18}F-FLT uptake was visible in nonproliferating tumors. ^{18}F-FLT PET may therefore be used for the differentiation of benign from malignant lung tumors.

However, 2 patients with NSCLC (1 case of carcinoma in situ and 1 of large cell carcinoma with low proliferative activity), and another patient with pulmonary metastases from colorectal cancer with a proliferation rate of 12%, showed no ^{18}F-FLT uptake but clear uptake of ^{18}F-FDG. Compared with ^{18}F-FDG, ^{18}F-FLT seems less sensitive for staging disease in patients with malignant lung tumors. Further studies with larger patient populations are needed to determine the diagnostic accuracy of ^{18}F-FLT PET in detecting malignant tumors.

Several studies have reported that ^{18}F-FDG PET can be used to assess therapeutic response in various tumors (*29–33*). A first in vitro study demonstrated that ^{18}F-FLT uptake in esophageal cancer cells was modified early after incubation with various cytotoxic drugs (*34*). Hence, ^{18}F-FLT may be an alternative for therapeutic monitoring. However, for evaluation of ^{18}F-FLT as a marker for therapy response, large clinical trials are needed.

CONCLUSION

^{18}F-FLT correlates significantly better with the proliferative activity of lung tumors than does ^{18}F-FDG. ^{18}F-FLT may therefore be the superior PET tracer for assessment of therapy response and outcome. Because of 3 false-negative findings in our preliminary study, ^{18}F-FLT PET may be less adequate than ^{18}F-FDG for primary staging in patients with known lung cancer but may be more accurate for differentiation of unclear lung lesions.

REFERENCES

1. Hicks RJ, Kalff V, MacManus MP, et al. ^{18}F-FDG PET provides high-impact and powerful prognostic stratification in staging newly diagnosed non-small cell lung cancer. *J Nucl Med.* 2001;42:1596–1604.
2. Kalff VV, Hicks RJ, MacManus M, et al. Clinical impact of (18)F fluorodeoxyglucose positron emission tomography in patients with non-small-cell lung cancer: a prospective study. *J Clin Oncol.* 2001;19:111–118.
3. Gould MK, Maclean CC, Kuschner WG, Rydzak CE, Owens DK. Accuracy of positron emission tomography for diagnosis of pulmonary nodules and mass lesions: a meta-analysis. *JAMA.* 2001;285:914–924.
4. Shreve PD, Anzai Y, Wahl RL. Pitfalls in oncologic diagnosis with FDG PET imaging: physiologic and benign variants. *Radiographics.* 1999;19:61–77.
5. Buck AC, Schirrmeister HH, Guhlmann CA, et al. Ki-67 immunostaining in pancreatic cancer and chronic active pancreatitis: does in vivo FDG uptake correlate with proliferative activity? *J Nucl Med.* 2001;42:721–725.
6. Dosaka-Akita H, Hommura F, Mishina T, et al. A risk-stratification model of non-small cell lung cancers using cyclin E, Ki-67, and ras p21: different roles of G1 cyclins in cell proliferation and prognosis. *Cancer Res.* 2001;61:2500–2504.
7. Vesselle H, Schmidt RA, Pugsley JM, et al. Lung cancer proliferation correlates with [F-18]fluorodeoxyglucose uptake by positron emission tomography. *Clin Cancer Res.* 2000;6:3837–3844.
8. Higashi K, Ueda Y, Yagishita M, et al. FDG PET measurement of the proliferative potential of non-small cell lung cancer. *J Nucl Med.* 2000;41:85–92.
9. Vansteenkiste JF, Stroobants SG, Dupont PJ, et al. Prognostic importance of the

standardized uptake value on (18)F-fluoro-2-deoxy-glucose-positron emission tomography scan in non-small-cell lung cancer: an analysis of 125 cases. Leuven Lung Cancer Group. *J Clin Oncol.* 1999;17:3201–3206.
10. Mac Manus MP, Hicks RJ, Ball DL, et al. F-18 fluorodeoxyglucose positron emission tomography staging in radical radiotherapy candidates with nonsmall cell lung carcinoma: powerful correlation with survival and high impact on treatment. *Cancer.* 2001;92:886–895.
11. Shields AF, Grierson JR, Kozawa SM, Zheng M. Development of labeled thymidine analogs for imaging tumor proliferation. *Nucl Med Biol.* 1996;23: 17–22.
12. Shields AF, Grierson JR, Dohmen BM, et al. Imaging proliferation in vivo with [F-18]FLT and positron emission tomography. *Nat Med.* 1998;4:1334–1336.
13. Rasey JS, Grierson JR, Wiens LW, Kolb PD, Schwartz JL. Validation of FLT uptake as a measure of thymidine kinase-1 activity in A549 carcinoma cells. *J Nucl Med.* 2002;43:1210–1217.
14. Buck AK, Schirrmeister H, Hetzel M, et al. 3-deoxy-3-[(18)F]fluorothymidine-positron emission tomography for noninvasive assessment of proliferation in pulmonary nodules. *Cancer Res.* 2002;62:3331–3334.
15. Machulla HJ, Blocher A, Kuntzsch M, et al. Simplified labeling approach for synthesizing 3′-deoxy-3′-[^{18}F]fluorothymidine ([^{18}F]FLT). *J Radioanal Nucl Chem.* 2000;24:843–846.
16. Schmidlin P. Iterative algorithms for emission tomography [in German]. *Nuklearmedizin.* 1990;3:155–158.
17. Marom EM, McAdams HP, Erasmus JJ, et al. Staging non-small cell lung cancer with whole-body PET. *Radiology.* 1999;212:803–809.
18. Vansteenkiste JF, Stroobants SG, De Leyn PR, et al. Lymph node staging in non-small-cell lung cancer with FDG-PET scan: a prospective study on 690 lymph node stations from 68 patients. *J Clin Oncol.* 1998;16:2142–2149.
19. Kubota R, Kubota K, Yamada S, Tada M, Takahashi T, Iwata R. Microautoradiographic study for the differentiation of intratumoral macrophages, granulation tissues and cancer cells by the dynamics of fluorine-18-fluorodeoxyglucose uptake. *J Nucl Med.* 1994;35:104–112.
20. Marom EM, Aloia TA, Moore MB, et al. Correlation of FDG-PET imaging with Glut-1 and Glut-3 expression in early-stage non-small cell lung cancer. *Lung Cancer.* 2001;33:99–107.
21. Brown RS, Leung JY, Kison PV, Zasadny KR, Flint A, Wahl RL. Glucose transporters and FDG uptake in untreated primary human non-small cell lung cancer. *J Nucl Med.* 1999;40:556–565.
22. Kubota K, Ishiwata K, Kubota R, et al. Tracer feasibility for monitoring tumor radiotherapy: a quadruple tracer study with fluorine-18-fluorodeoxyglucose or fluorine-18-fluorodeoxyuridine, L-[methyl-^{14}C]methionine, [6-^{3}H]thymidine, and gallium-67. *J Nucl Med.* 1991;32:2118–2123.
23. Bos R, van Der Hoeven JJ, van Der Wall E, et al. Biologic correlates of (18)fluoro-deoxyglucose uptake in human breast cancer measured by positron emission tomography. *J Clin Oncol.* 2002;20:379–387.
24. Avril N, Menzel M, Dose J, et al. Glucose metabolism of breast cancer assessed by ^{18}F-FDG PET: histologic and immunohistochemical tissue analysis. *J Nucl Med.* 2001;42:9–16.
25. Eary JF, Mankoff DA, Spence AM, et al. 2-[C-11]thymidine imaging of malignant brain tumors. *Cancer Res.* 1999;59:615–621.
26. Conti PS, Alauddin MM, Fissekis JR, Schmall B, Watanabe KA. Synthesis of 2′-fluoro-5-[^{11}C]-methyl-1-beta-D-arabinofuranosyluracil ([^{11}C]-FMAU): a potential nucleoside analog for in vivo study of cellular proliferation with PET. *Nucl Med Biol.* 1995;22:783–789.
27. Blasberg RG, Roelcke U, Weinreich R, et al. Imaging brain tumor proliferative activity with [^{124}I]iododeoxyuridine. *Cancer Res.* 2000;60:624–635.
28. Mier W, Haberkorn U, Eisenhut M. [^{18}F]FLT: portrait of a proliferation marker. *Eur J Nucl Med Mol Imaging.* 2002;29:165–169.
29. Hoekstra CJ, Hoekstra OS, Stroobants SG, et al. Methods to monitor response to chemotherapy in non-small cell lung cancer with ^{18}F-FDG PET. *J Nucl Med.* 2002;43:1304–1309.
30. Spaepen K, Stroobants S, Dupont P, et al. Early restaging positron emission tomography with (18)F-fluorodeoxyglucose predicts outcome in patients with aggressive non-Hodgkin's lymphoma. *Ann Oncol.* 2002;13:1356–1363.
31. Flamen P, Van Cutsem E, Lerut A, et al. Positron emission tomography for assessment of the response to induction radiochemotherapy in locally advanced oesophageal cancer. *Ann Oncol.* 2002;13:361–368.
32. Spence AM, Muzi M, Graham MM, et al. 2-[(18)F]Fluoro-2-deoxyglucose and glucose uptake in malignant gliomas before and after radiotherapy: correlation with outcome. *Clin Cancer Res.* 2002;8:971–979.
33. Weber WA, Ott K, Becker K, et al. Prediction of response to preoperative chemotherapy in adenocarcinomas of the esophagogastric junction by metabolic imaging. *J Clin Oncol.* 2001;19:3058–3065.
34. Dittmann H, Dohmen BM, Kehlbach R, et al. Early changes in [(18)F]FLT uptake after chemotherapy: an experimental study. *Eur J Nucl Med Mol Imaging.* 2002;29:1462–1469.

JNM The Journal of NUCLEAR MEDICINE

Imaging Proliferation in Lung Tumors with PET: ^{18}F-FLT Versus ^{18}F-FDG

Andreas K. Buck, Gisela Halter, Holger Schirrmeister, Jörg Kotzerke, Imke Wurziger, Gerhard Glatting, Torsten Mattfeldt, Bernd Neumaier, Sven N. Reske and Martin Hetzel

J Nucl Med. 2003;44:1426-1431.

The Journal of Nuclear Medicine is published monthly.
SNMMI | Society of Nuclear Medicine and Molecular Imaging
1850 Samuel Morse Drive, Reston, VA 20190.
(Print ISSN: 0161-5505, Online ISSN: 2159-662X)

SNMMI SOCIETY OF NUCLEAR MEDICINE AND MOLECULAR IMAGING